Theory of structural phase transitions in crystalline poly(vinylidene fluoride)

N. C. Banik, F. P. Boyle, T. J. Sluckin, P. L. Taylor, S. K. Tripathy et al.

Citation: J. Chem. Phys. **72**, 3191 (1980); doi: 10.1063/1.439552
View online: http://dx.doi.org/10.1063/1.439552
View Table of Contents: http://jcp.aip.org/resource/1/JCPSA6/v72/i5
Published by the AIP Publishing LLC.

Theory of structural phase transitions in crystalline poly(vinylidene fluoride)

N. C. Banik, F. P. Boyle,[a] T. J. Sluckin,[b] and P. L. Taylor

Department of Physics, Case Western Reserve University, Cleveland, Ohio 44106

S. K. Tripathy and A. J. Hopfinger

Department of Macromolecular Science, Case Western Reserve University, Cleveland, Ohio 44106
(Received 17 September 1979; accepted 14 November 1979)

A mean-field theory capable of predicting structural phase transitions in a linear polymer is presented. The intrachain and interchain potentials, derived from conformational analysis based upon molecular mechanics, are combined in a transfer-integral approach to calculate free energies as a function of temperature and applied uniaxial stress. The theory is applied to poly(vinylidene fluoride) and is successful in yielding several observed phases of this material and in predicting the effect of uniaxial stress on the most stable phase. There are no adjustable parameters in the theory.

I. INTRODUCTION

The discovery[1] that poly(vinylidene fluoride), also known as PVF_2, can exhibit very large piezoelectric and pyroelectric effects has prompted many investigators[2] to make a comprehensive study of this interesting polymer. The particular crystalline phase in which PVF_2 shows these effects is called phase I, or the β phase, and is only one of at least three crystalline phases in which the polymer is known to exist. Phase II, or the α phase, is probably the most stable low-temperature phase, and is grown very readily from the melt. The β phase is produced by stretching a film of α phase under appropriate conditions. Phase III, or the γ phase, can be produced from the melt under very high pressure. While the crystal structures and the chain conformations of the first two phases are well established, those for the third phase are still a matter of discussion.

The purpose of this paper[3] is to present a mean-field theory that can predict, in a polymer, the existence of multiple phases and their relative stabilities as a function of temperature and uniaxial stress. A simple version of the theory is applied to study PVF_2. The simple theory, which has no adjustable parameters, is successful in yielding several observed phases of the polymer and in predicting the effect of uniaxial stress on the most stable phase.

In two previous papers,[4] henceforth called I and II, a theory was presented to calculate the free energy of two simple polymers (polyethylene and polytetrafluoroethylene) as a function of temperature: In these calculations both intrachain and interchain interactions were included. The basic approach was to calculate with some precision the statistical mechanics of a single chain by means of a transfer-integral (TI) formalism and then to approximate the interchain interactions in terms of mean fields determined self-consistently from the interaction potentials. The central quantities considered in these calculations were the distribution $n(\theta)$ of the torsional angles along a chain and its temperature variation in equilibrium. Calculations were carried out under the constraint of a fixed valence geometry. The classical partition function for an isolated chain of N monomer units was shown, in the thermodynamic limit, to tend to λ_m^N, where λ_m is the largest eigenvalue of the TI equation

$$\lambda\psi(\theta) = \frac{1}{2\pi}\int \exp[-\beta \mathfrak{u}(\theta,\theta')\psi(\theta')d\theta'] \ , \tag{1}$$

with β the inverse temperature $(kT)^{-1}$, and where $\mathfrak{u}(\theta,\theta')$ is the change in potential energy on adding to a chain whose last torsional angle is θ', a further unit at angle θ. The kinetic energy is assumed to separate and is excluded from the free energy derived from the partition function. The distribution $n(\theta)$ is related to ψ through the relation

$$n(\theta) = \psi^2(\theta) \Big/ \int \psi^2(\theta')d\theta' \ . \tag{2}$$

The mean-field approximation for the interchain interaction resides in the assumption that the contribution of interchain forces to the energy per monomeric unit can be written as a functional $V_2[n(\theta)]$ of the $n(\theta)$ alone. This yields a soluble set of equations for the free energy of the system through the introduction of the fictitious mean field $h(\theta)$, defined through the relation

$$h(\theta) = (\delta V_2/\delta n) \ . \tag{3}$$

This procedure is equivalent to solving for the free energy of a simple isolated chain as a functional of $n(\theta)$, and then searching for absolute and local minima of the total free energy $\mathfrak{F}$ of the interacting system, defined as

$$\mathfrak{F}[n(\theta)] = \mathfrak{F}_0[n(\theta)] + V_2[n(\theta)] \ . \tag{4}$$

The above concepts are extended in Sec. II to introduce additional correlations between adjacent torsional angles along the chain. This enables the theory to predict structures in which the repeat unit along the chain contains two successive torsional states. The formalism is general and can be applied to any crystalline polymer with linear chain molecules. In this paper, however, we are interested in applying the theory to

[a] Present address: Materials Research Division, Gould Inc., Cleveland, OH 44108.

[b] Present address: H. H. Wills Physics Laboratory, University of Bristol, Bristol BS8 1TL, United Kingdom.

 0021-9606/80/053191-06$01.00

poly(vinylidene fluoride). This is done by introducing an additional constraint of fixing the alternate torsional angles at *trans* as discussed in Sec. III.

The molecular energetics needed in the calculation are obtained using conformational analysis. This is discussed in some detail in Sec. IV. The results of the calculation of the free energy are discussed in Sec. V. We find that the theory can predict all the phases of PVF_2 that have been observed experimentally. The prediction of the melting temperature of the most stable α phase and the effects of uniaxial stress on this phase are in reasonable agreement with the experiment.

II. FORMALISM

We consider a linear array of N torsional angles ($N+2$ bonds) connecting the monomer units of a chain. M such chains constitute the polymeric system under consideration. We divide the array into two sublattices θ_{2i} and θ_{2i+1} which we call the A and B sublattices, respectively. We allow the distributions $n_A(\theta)$ and $n_B(\theta)$ on these sublattices to differ. The intrachain contribution to the Hamiltonian is then written in the form

$$V_1 = \frac{MN}{2}\int \mathfrak{u}(\theta,\theta')[n_{AB}(\theta,\theta')+n_{BA}(\theta,\theta')]d\theta\, d\theta' \,. \tag{5}$$

The joint distribution $n_{AB}(\theta,\theta')$ measures the probability that a pair of torsional angles at adjacent sites A and B will be found at θ and θ', respectively. The function $\mathfrak{u}(\theta,\theta')$ has been defined in Sec. I.

The interchain energy is written in the form

$$V_2 = \frac{NMz}{2}\int W(\theta_1,\theta_1',\theta_2,\theta_2')n_A(\theta_1)n_B(\theta_1')n_A(\theta_2) \times n_B(\theta_2')d\theta_1 d\theta_1' d\theta_2 d\theta_2' \,, \tag{6}$$

where z is the number of nearest neighbor chains in the crystalline lattice. The function $W(\theta_1,\theta_1'.\theta_2,\theta_2')$ is defined as the potential energy of a monomeric unit located in a chain segment of torsional angles θ_1 and θ_1' in the potential of another chain segment with angles θ_2 and θ_2'. The essence of the mean-field approximation lies in the assumption that V_2 can be written as a functional of n_A and n_B alone; correlations between chains are thus neglected. The interchain parameters—the distance between chains, the relative orientation between chain axes, and the relative positions of the A and B sublattice sites in the neighboring chains—are not variables in this simple thoery, but are determined merely by minimization of W with respect to these variables. The minimization procedure is discussed in detail in Sec. III. The method has the advantage that no prior knowledge of the crystal structure is necessary in the calculation. In fact, the lattice parameters are obtained as a byproduct in the process of calculating W. However, since only two chains are considered in the present calculation, these lattice parameters are not likely to be very reliable. The consideration of more than two chains will be discussed in a future publication.

We also consider the application of a uniaxial stress along the direction of the chain axis. This we do by adding an extra term to the Hamiltonian in the form

$$V_3 = -\phi M\sum_i [a(\theta_A)+a(\theta_B)] \,. \tag{7}$$

Here, ϕ is an effective stress force and $a(\theta)$ is a normalized length function. The stress parameter ϕ can be related to the physical stress by considering the dimensions of the unit cell of the crystalline lattice.

By means of the arguments given in I and II, the mean fields $h_A(\theta)$ and $h_B(\theta)$ can be related to the interchain energy V_2 in the following way: We write an effective intrachain Hamiltonian

$$H_{\text{eff}} = \frac{NM}{2}\iint [V_{AB}(\theta,\theta')n_{AB}(\theta,\theta') + V_{BA}(\theta,\theta')n_{BA}(\theta,\theta')]d\theta\, d\theta' \,, \tag{8}$$

where

$$V_{AB}(\theta,\theta') = \mathfrak{u}(\theta,\theta') + \tfrac{1}{2}[h_A(\theta)+h_B(\theta')] - \frac{\phi}{2}[a(\theta)+a(\theta')] \,, \tag{9}$$

$$V_{BA}(\theta,\theta') = \mathfrak{u}(\theta,\theta') + \tfrac{1}{2}[h_A(\theta')+h_B(\theta)] - \frac{\phi}{2}[a(\theta)+a(\theta')] \,.$$

Consequently, the TI equations are

$$\begin{aligned}\lambda\psi_A(\theta) &= \int d\theta'\psi_A(\theta')\int d\theta''\, \exp\{-\beta[V_{AB}(\theta',\theta'') + V_{BA}(\theta'',\theta)]\} \\ \lambda\psi_B(\theta) &= \int d\theta'\psi_B(\theta')\int d\theta''\exp\{-\beta[V_{BA}(\theta',\theta'') + V_{AB}(\theta'',\theta)]\} \,.\end{aligned} \tag{10}$$

The classical partition function in the thermodynamic limit is obtained from the largest eigenvalue of the above equations. It can also be verified that

$$\begin{aligned} n_A(\theta) &= \psi_A(\theta)\bar{\psi}_A(\theta)\Big/\int \psi_A(\theta)\bar{\psi}_A(\theta)d\theta \,, \\ n_B(\theta) &= \psi_B(\theta)\bar{\psi}_B(\theta)\Big/\int \psi_B(\theta)\bar{\psi}_A(\theta)d\theta \,, \end{aligned} \tag{11}$$

with ψ_A and ψ_B the eigenfunctions corresponding to the largest eigenvalue λ and $\bar{\psi}_A, \bar{\psi}_B$ the corresponding eigenfunctions of the transposed equations. The Gibbs energy per monomer unit is then given by

$$G = -\tfrac{1}{2}k_BT\ln\lambda - \tfrac{1}{2}\int [h_A(\theta)n_A(\theta)+h_B(\theta)n_B(\theta)]d\theta + V_2. \tag{12}$$

This is minimized with respect to $n_A(\theta)$ and $n_B(\theta)$, leading to the relations

$$\begin{aligned} h_A(\theta) &= 2\delta V_2[n_A,n_B]/\delta n_A \,, \\ h_B(\theta) &= 2\delta V_2[n_A,n_B]/\delta n_B \,. \end{aligned} \tag{13}$$

We then have an iterative method to derive solutions for Eqs. (9) to (13). First a reasonable guess for a trial solution for $n_A(\theta)$ and $n_B(\theta)$ is made and then $h_A(\theta)$ and $h_B(\theta)$ are derived from Eq. (13), which in turn define the effective intrachain energy in Eq. (9). Then from Eqs. (10) and (11) new $n_A(\theta)$ and $n_B(\theta)$ are obtained. The process is continued until self-consistent solutions for $n_A(\theta)$ and $n_B(\theta)$ are found. If more than one such set of solu-

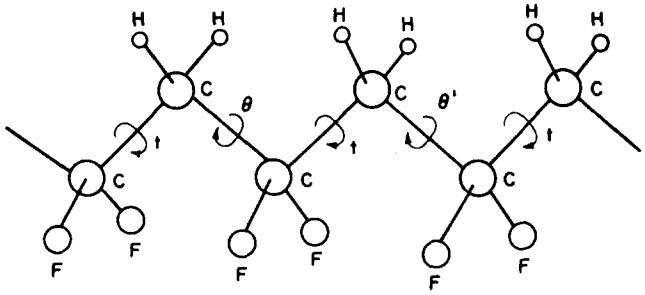

FIG. 1. Molecular structure of poly(vinylidene fluoride). The torsional angles marked t are constrained to be zero and those marked θ, θ' are allowed to vary.

tions exist, the true stable solution is the one with the lowest Gibbs energy, while the others are metastable.

III. APPLICATION TO PVF_2

In the α phase of PVF_2, the equilibrium chain conformation is known to have a repeat unit of four torsional angles *trans–gauche–trans–gauche'*. There are thus correlations present of longer range than can emerge from the next nearest neighbor formalism described in Sec. II. Indeed, in order correctly to describe this phase it would be necessary to include four distinct distributions $n_A(\theta), n_B(\theta), n_C(\theta)$, and $n_D(\theta)$ to specify the four torsional distributions within an α-phase unit cell. It would also be necessary to construct an interchain energy functional W of all these distributions. In order to avoid this complexity and yet still construct a realistic picture of PVF_2, we have chosen a simpler model which makes use of the fact that the large electrostatic repulsion between fluorine atoms makes it energetically unfavorable for *gauche* or *gauche'* conformations to follow either *gauche* or *gauche'* along a chain, that is to say, each *gauche* or *gauche'* conformation is most probably followed by a *trans* conformation. The model we adopt incorporates this fact by fixing every second bond to be *trans* and allowing rotations to occur only about alternate bonds, which are not so constrained. In what follows, then, θ_{4i} refers to an A site and θ_{4i+2} to a B site, with θ_{4i+1} and θ_{4i+3} fixed at *trans*; the degrees of freedom of the system are the torsional angles between successive CH_2CF_2 monomer units. This picture is consistent with the known structure of the α and β phases as well as with two recently conjectured structures[5–7] for the γ phase, also known as phase III. The model is illustrated in Fig. 1. The weakness of the model lies in its inability to describe crystal structures having larger repeat units and in the fact that it is not completely appropriate to describe the melt, in which the identity of A and B sites is presumably lost.

Although the formalism has been expressed in terms of the continuously variable angles θ, all the energies $u(\theta, \theta')$ and $W(\theta_1, \theta_1', \theta_2, \theta_2')$ are calculated numerically using conformational analysis. Consequently, it is impossible to use analytic methods of the type used by other authors[8] in simpler models to solve the TI equations. The integrations over angles θ must necessarily be replaced by summations over a grid of m uniformly spaced discrete values; in this way the continuum model is replaced by what has been called an m-state model. In I, we considered the cases $m = 3, 6, 12$, and 24, the last two cases being very good approximations to the continuum theory.

In I the interchain interaction was a function of only two arguments, whereas in this calculation the interchain interaction is a function of four arguments. This magnifies enormously the amount of computation necessary to calculate even one value of $W(\theta_1, \theta_2, \theta_1', \theta_2')$ and there are now of the order of n^4 such values required. In this calculation, we compromise between the ideal of large m and the computational difficulties by taking $m = 6$. The transfer integral is then reduced to a 6×6 matrix. In this connection, it may be mentioned that in I the use of larger matrices was found to give results qualitatively similar to, but with a lower melting point than, the 6×6 approximation. We would expect a similar trend in the present case, because the intrachain energy map, which is shown in Fig. 2, contains minima at $\theta, \theta' = 0°$, 120°, and 240°. This has also been verified in the oversimplified 3×3 approximation.

The function $a(\theta)$ in Eq. (7) is the normalized length of a chain segment containing the torsional angle θ. In the present model of PVF_2, in which we keep alternate torsional angles fixed at *trans*, we choose to define it as the distance between a carbon atom and its fourth nearest neighbor along a chain, so that

$$a(\theta) = (1 - \cos^2\tfrac{1}{2}\psi \sin^2\tfrac{1}{2}\theta)^{1/2} . \tag{14}$$

The angle $\psi = 114°$ is the C–C–C bond angle. The stress-energy term given in Eq. (7) tends to maximize $a(\theta)$ and consequently to favor the *trans* conformation.

IV. MOLECULAR ENERGETICS

Both intra- and interchain molecular energetics were computed in the same manner as reported for polymethylene and polytetrafluoroethylene in I and II. A molecular mechanics potential,[9] as embodied in our molecular

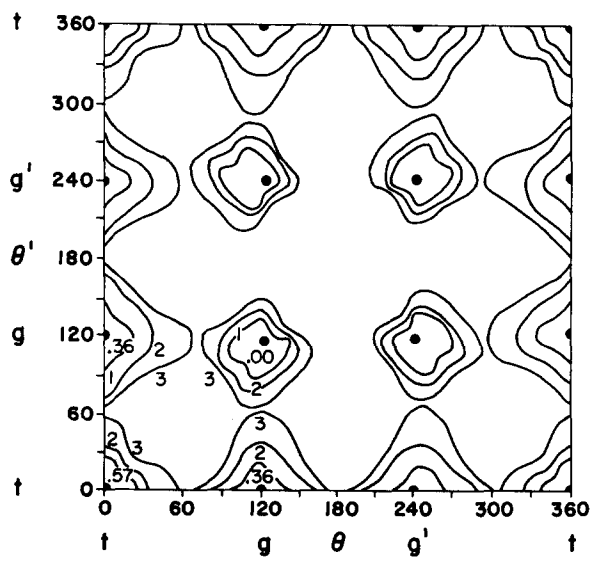

FIG. 2. Polar plot of intrachain energy for poly(vinylidene fluoride) as a function of θ and θ'.

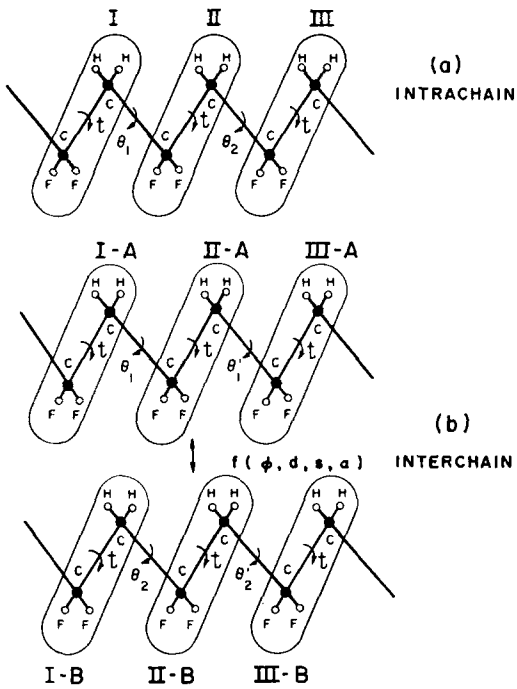

FIG. 3. Schematic grouping of atoms in PVF_2 chains as described in the text (Sec. IV) to discuss the calculation of potential energy functions: (a) for intrachain energy; (b) for interchain energy.

structure calculator CAMSEQ-II,[10] was used to determine the molecular energetics. The partial atomic charges were computed using the CNDO/2 molecular orbital method.[11] The valence geometry determined in the x-ray structural analysis of PVF_2 was adopted in the conformational analyses.

The group interaction partitioning used in the conformational analyses to facilitate accommodation into the statistical mechanics formalism is shown in Fig. 3. The I–II(θ_1) and I–III(θ_1, θ_2) interchain interactions were explicitly considered. The group interchain interactions determined are (I-*A*)–(I-*B*), (I-*A*)–(II-*B*), and (I-*A*)–(III-*B*) for particular choices of θ_1, θ_1' and θ_2, θ_2'. These group interactions correspond to the interchain geometry as governed by $f(\phi, d, S, \alpha)$ for which the total energy is minimized. Here, ϕ is the rotation of one chain about the other, d is the interchain separation distance, S is a translation of one chain along its axis relative to the other chain, and α is a rotation of a chain about its own chain axis. All interchain energy calculations included the constraint of having the two chain axes parallel for all configurations.

V. RESULTS AND DISCUSSION

The results of these calculations suggest the existence of at least five different stable or metastable phases of PVF_2 as indicated by the local minima in the Gibbs energy as a functional of the distributions $n_A(\theta)$ and $n_B(\theta)$. Each of these phases is characterized by the temperature range over which it is stable or metastable. We consider first the case of zero applied stress.

Figure 4 shows the Helmholtz energy as a function of temperature, with the various phases found in the calculation labeled $\alpha, \beta, \gamma, \delta$, and m. Because the intrachain potential energy has deep minima at $\theta = 0$ (designated t), at $\theta = 2\pi/3$ (designated g), and $\theta = 4\pi/3$ (designated g'), the various distributions n_A and n_B are localized around these values; the distributions can be characterized by a set of numbers $n_i^p(\theta)$, with $i = A, B$; $p = \alpha, \beta, \gamma, \delta, m$; $\theta = t, g, g'$. Thus, for example, $n(g) = \int_{\pi/3}^{\pi} n(\theta) d\theta$. This allows us to show the form of the various n in Fig. 5, in which $n(g)$ is plotted as the abscissa and $n(g')$ the ordinate; $n(t)$ is then $1 - n(g) - n(g')$.

The most stable low-temperature phase at zero stress is that labeled α, and has $n_A^\alpha(g') = n_B^\alpha(g) = 1$ at zero temperature. The chain conformation, including the alternate angles assumed fixed at t, then is of the form *tgtg'*. This is, therefore, the experimentally known phase II, or α phase. The second low-temperature phase has $n^\beta(g) = n^\beta(g') = 0$ at zero temperature. The chain conformation of this phase, therefore, is *tttt*, and this is the all-*trans* polar phase I, or β phase. This phase is higher in free energy than the α phase and thus only metastable throughout its temperature range. The high-temperature phase m has $n_A(\theta) = n_B(\theta) = n(\theta)$, and approaches equal values for $n(t)$, $n(g)$, and $n(g')$ as the temperature becomes very large. We identify this with the melt phase.

The phases marked γ and δ have the chain structures *tttg* (or *tttg'*) and *tgtg* (or *tg'tg'*), respectively. These are the highest in free-energy and hence most unstable. Their possible existence has not yet been verified experimentally.

The calculation suggests that in equilibrium a first-order phase transition should take place between the α phase and the melt at $T = 513$ K, where the free energies of the two phases cross in Fig. 4. Although the free energies of the β phase and the melt also cross at 414 K, this does not necessarily correspond to a phase transition from β to melt or *vice versa* because the free ener-

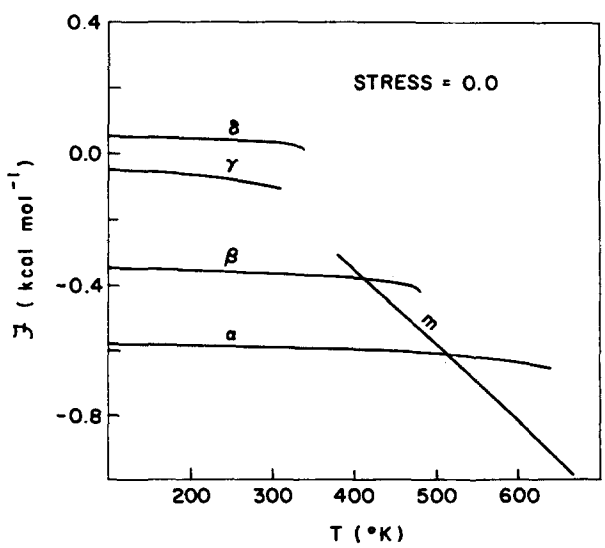

FIG. 4. Plot of the local minima in the Helmholtz energy as a function of temperature. The termination of each line represents the limit of metastability of that phase.

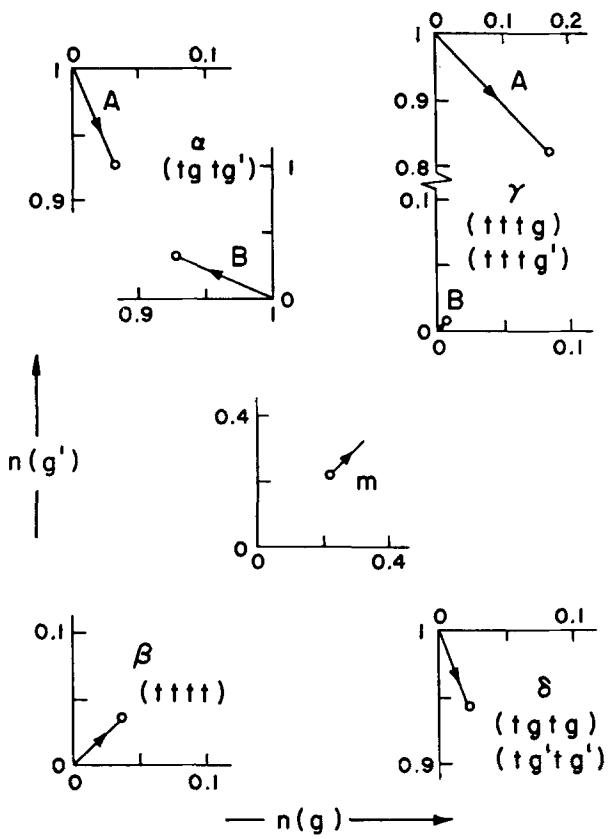

FIG. 5. This set of diagrams describes the predicted chain conformation of each phase of PVF_2 and its change with temperature. The quantities $n(g)$ and $n(g')$, the fraction of torsional angles near 120° and 240°, respectively, are plotted for each phase shown in Fig. 4. Values for each sublattice A and B are shown when they differ. The arrows indicate the direction of increasing temperature and the open circles mark points of absolute instability.

gy of the α phase is lower than that of the melt in this temperature region. With the increase of temperature, the β phase may convert into the α phase before going into the melt. Similarly, if one starts from the melt and lowers the temperature, the β phase may be reached only by supercooling. The β phase is predicted to be absolutely unstable at $T \simeq 500$ K following the disappearance of this minimum from the plot of free energy. At this temperature the β phase must transform into a state of lower free energy, namely, the melt or the α phase.

The experimental situation[12] appears to be that both the α phase and β phase melt at about 460 K, and that the α phase crystallizes more readily out of the melt than the β phase. The latter fact strongly suggests that the free energy of the α phase near the melting temperature is lower than that of the β phase. This is in agreement with our prediction.

The predicted melting temperature is around 50 K higher than that observed experimentally. However, in view of the mean-field nature of our theory, a higher melting temperature is not unexpected.

The entropy change on melting of the α phase is predicted to be 2.18 cal $mol^{-1} K^{-1}$, which may be compared with the experimental value[12] of around 3.16 cal $mol^{-1} K^{-1}$. The discrepancy may be a result of the fact that we calculate only the configurational part of the entropy, the phonon part being neglected in the present calculation. The coarseness of the six-state model, which neglects some of the effects of the shape of the potential wells, may also contribute to this discrepancy.

The prediction of the two high-energy metastable phases γ with chain conformation *tttg* (or *tttg'*) and δ with chain conformation *tgtg* (or *tg'tg'*) result from the very low intrachain energy of these conformations. However, the interchain energy for these conformations is very high. The presence of these phases in our results may arise from the mean-field approximation of the interchain potentials which averages over the interchain potentials. It is also possible that the consideration of more than two chains in calculating the interchain energy would shed more light on the existence of these phases. Another point to note in this connection is that in the expression for V_2 [Eq. (6)] it is assumed that two neighboring chains are in register. This means that an A site in one chain has an A site as its closest neighbor in the other chain. This need not be true. For example, in the α phase of PVF_2, it is known that one chain is laterally translated with respect to the other by about half a monomer unit. The consequence of this translation is partially accounted for in the procedure of minimizing the interchain energy as discussed in Sec. IV. In the formal theory we can consider only the most extreme case, i.e., the case where an A site in one chain has a B site as its closest neighbor in the other chain. Equation (6) will then be replaced by

$$V_2 = \frac{NMz}{2} \int W(\theta_1, \theta_1', \theta_2, \theta_2') n_A(\theta_1) n_B(\theta_1') n_B(\theta_2) \times n_A(\theta_2') d\theta_1 d\theta_2 d\theta_1' d\theta_2 \,. \tag{15}$$

The calculation was repeated with this expression substituted for the original form of V_2, with the result that the melt transition temperature for the α phase was

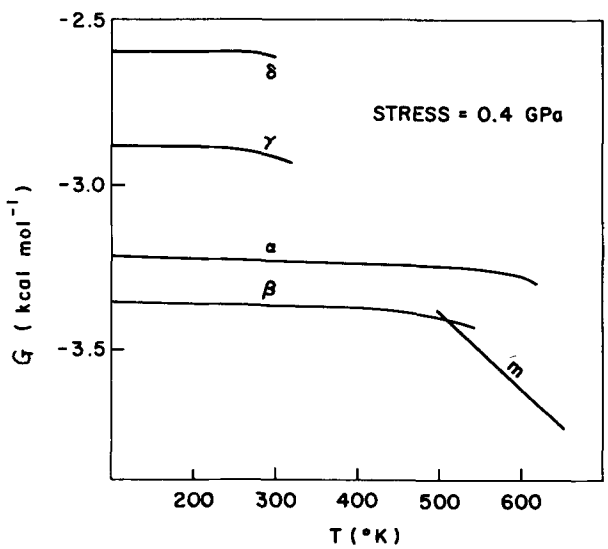

FIG. 6. The same plot as Fig. 4, but at a finite uniaxial stress.

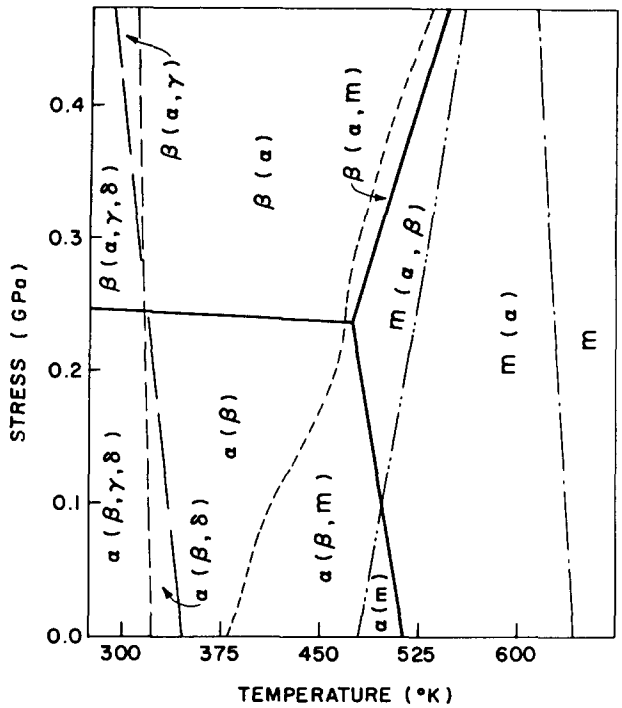

FIG. 7. Uniaxial stress-temperature phase diagram for PVF_2 predicted by the theory. The solid lines show the regions of stability of the phases α, β, and m. The broken lines separate regions of metastability, with the possible metastable phases shown in parentheses.

reduced to 450 K, which is very close to the experimental value of 460 K. It is also found that the chain conformation of the γ phase is changed to *trans–trans–trans*–50% *gauche* and 50% *gauche'*. Interestingly, this conformation is completely compatible with one of the conformations *tttgtttg'* that was proposed[6,7] for the experimental γ phase of Weinhold, Litt, and Lando.[5]

We now turn to the situation where a finite uniaxial stress is applied. As might be expected, the effect of the applied stress is to destabilize the α phase in favor of the more extended β phase. Sample results are shown in Fig. 6, in which the Gibbs free energy is plotted as a function of temperature at a stress of 0.4 GPa. We obtain a structural phase transition from the α phase to the β phase as a function of applied stress.

The richness of the theory in predicting the existence of different phases with their stabilities as a function of temperature and stress is illustrated in Fig. 7. In this figure each region is labeled with the most stable phase, with possible metastable phases in parentheses. That there are regions corresponding to the melt at finite stress is an artefact of the model, in which stress is the variable conjugate to chain length.

There are a number of predictions that one can make from the phase diagram in Fig. 7. For example, as we increase the applied uniaxial stress, the melting point of the α phase is lowered, while that of the β phase is increased. Also, the amount of stress necessary to initiate an $\alpha \rightarrow \beta$ phase transition decreases with increasing temperature.[13] Because of a lack of experimental data, one can not readily verify these and other predictions of the theory. One can only hope that this work will encourage further experimental investigation in the future.

ACKNOWLEDGMENTS

This work was supported in part by the Army Research Office through Grant DAAG 29-78G-0064 and by the Materials Research Laboratory Program of the National Science Foundation through Grant DMR 76-80710. We acknowledge fruitful discussion with Dr. W. M. Prest, Jr. of Xerox Webster Research Center, Rochester, NY. PLT thanks the Los Alamos Scientific Laboratory, where part of this work was performed, for their hospitality.

[1]H. Kawai, Jpn. J. Appl. Phys. **8**, 975 (1969).
[2]For a list of references see, for example, R. G. Kepler, Annu. Rev. Phys. Chem. **29**, 497 (1978).
[3]A brief report of this work was given by N. C. Banik, F. P. Boyle, T. J. Sluckin, P. L. Taylor, S. K. Tripathy, and A. J. Hopfinger in Phys. Rev. Lett. **43**, 456 (1979).
[4]F. P. Boyle, P. L. Taylor, and A. J. Hopfinger, J. Chem. Phys. **67**, 353 (1977); **68**, 4730 (1978).
[5]S. Weinhold, M. H. Litt, and J. B. Lando, J. Polym. Sci. Polym. Lett. **17**, 585 (1979).
[6]N. C. Banik, P. L. Taylor, S. K. Tripathy, and A. J. Hopfinger, Macromolecules **12**, 1015 (1979).
[7]M. A. Bachmann, W. L. Gordon, J. L. Koenig, and J. B. Lando, J. Appl. Phys. **50**, 6106 (1979).
[8]See, for example, D. J. Scalapino, M. Sears, and R. A. Ferrell, Phys. Rev. B **6**, 3409 (1972).
[9]A. J. Hopfinger, *Conformational Properties of Macromolecules* (Academic, New York, 1973).
[10]R. Potenzone, Jr., E. Cavicchi, H. J. R. Weintraub, and A. J. Hopfinger, Comput. Chem. **1**, 187 (1977).
[11]J. A. Pople and D. C. Beveridge, *Approximate Molecular Orbital Theory* (McGraw-Hill, New York, 1970).
[12]G. J. Welch, J. Polym. Sci. Polym. Phys. **14**, 1683 (1976).
[13]The data of B. P. Kosmynin, Ye L. Gal'perin, and D. Ya. Tsvankin, Vysokomol. Soyed. **6**, 1254 (1970) [English Translation: Polym. Sci. USSR A **12**, 1418 (1970)] apparently contradict this prediction. However, these data were taken on unoriented or poorly oriented samples. As those authors themselves suggested, the increase in temperature might cause an increase in the degree of orientation of the α phase crystallites, thus requiring more stress to cause an $\alpha \rightarrow \beta$ transformation. Since the theory presented here applies to crystalline samples, only data on highly oriented samples would be relevant in making comparisons with our predictions.